

## A Method for Correcting Vertical Velocities Measured from a Vessel-Mounted Acoustic Doppler Current Profiler

R. F. MARSDEN

*Physics Department, Royal Military College of Canada, Kingston, Ontario, Canada*

Y. GRATTON

*INRS-Océanologie, Rimouski, Quebec, Canada*

17 June 1996 and 24 March 1997

### ABSTRACT

Minor alignment errors ( $\sim 1^\circ$ ) can contaminate acoustic Doppler current profiler measurements of vertical velocities taken from a ship traveling at speed. The signature is consistently large positive or negative vertical velocities, recorded at all depths. A technique is proposed to postcorrect contaminated data in cases of tidally dominated flow over a flat bottom. The eigenmodes of the cross-correlation matrix of the depth-averaged velocities are found, and the data are rotated to align along the eigenvector corresponding to the smallest eigenvalue that is equivalent to the physical vertical direction. An example of corrupted data is presented, and corrections for the pitch and roll directions are found. The corrected flow field is shown to be physically plausible over both flat and sloping bottom sections of the cruise track.

### 1. Introduction

In recent years the acoustic Doppler current profiler (ADCP) has taken an increasingly important role in the detection of ocean currents. Of great importance is its ability to detect vertical velocities. This has proven essential in the identification of vertical convection, upwelling, and internal waves at tidal and higher frequencies. Schott and Leaman (1991) moored an upward-looking 75-kHz ADCP in the Gulf of Lyons and, through averaging the data over 1 h, were able to detect significant negative fluctuations in the vertical velocity that appeared to coincide with the onset of a major convection event. Marsden et al. (1994) mounted a downward-looking ADCP through land-fast ice in the Canadian Arctic Archipelago and, using the vertical velocity signal, identified internal waves propagating under land-fast ice. Marsden et al. (1995) further exploited the vertical velocity structure to calculate internal wave directional spectra using techniques similar to those proposed by Marsden and Juszko (1987) for surface gravity waves.

Both Schott and Leaman (1991) and Marsden et al. (1994) deployed their instruments in configurations that were essentially immobile with respect to the mean flow.

Consequently, minor alignment errors in the ADCP would not influence the vertical velocity. Consider, however, a vessel-mounted (VM) ADCP that is misaligned by an angle  $\theta$  with respect to the vertical. The apparent vertical velocity ( $w'$ ) is given by

$$w' = -u \sin\theta + w \cos\theta, \quad (1)$$

where  $u$  and  $w$  are the actual horizontal and vertical velocities, respectively. A slightly misaligned but stationary ADCP can produce reasonable estimates of the vertical velocity. For example, a  $1^\circ$  misalignment and a  $0.4 \text{ m s}^{-1}$  current will produce an error of  $7 \text{ mm s}^{-1}$ , which would be in the noise level (e.g., order  $1 \text{ cm s}^{-1}$ ) of typical ADCP measurements. Problems can arise, however, when an ADCP is even slightly misoriented on a moving ship. In an axis system fixed to the ship, the apparent vertical velocity is given by

$$\begin{aligned} w' &= -(u + U) \sin\theta + w \cos\theta \\ &= -u \sin\theta + w \cos\theta - U \sin\theta, \end{aligned}$$

where  $U$  is the speed of the water relative to the ship and is of uniform negative sign in the pitch direction. Since  $U \sin\theta$  dominates, a signature of misalignment is a large vertical velocity of uniform sign from the surface to the bottom depending on whether the pitch error is fore or aft ( $\sin\theta$  above). For a ship moving at  $4.0 \text{ m s}^{-1}$ , the  $1^\circ$  orientation error in the pitch direction will induce a  $7.0 \text{ cm s}^{-1}$  spurious signal in the vertical velocity, above the expected noise level of the instrument.

A 150-kHz ADCP was deployed from a moving ves-

---

*Corresponding author address:* Dr. R. F. Marsden, Physics Department Royal Military College of Canada, Kingston, ON K7K 5L0, Canada.  
E-mail: marsden@hp.rmc.ca

sel during the “couplage des processus physiques et biogéochimiques” (coupled physical and biogeochemical processes or COUPPB) study of water properties at the head of the Laurentian Channel in the St. Lawrence River estuary, near the confluence of the Saguenay River. One aim of the project was to assess the ability of topographic features to generate high-frequency internal waves, solitons, and hydraulic jumps. Consequently, accurate measurement of the vertical velocity was essential. In this paper, a method is proposed to postcorrect ADCP transducer misalignment by reorienting the velocity field along axes determined from the data. The vertical direction is taken to coincide with the direction of the eigenvector corresponding to the minimum eigenvalue of the velocity cross-correlation matrix. An example of data resulting from sensor misalignment is shown and the proposed correction to the section is applied, eliminating the large vertical velocities. The rotated vertical velocity field then contains considerable information on potential internal wave generation regions. The concept of applying realistic constraints to postcorrect ADCP data is not new. Joyce (1989) used ship velocities obtained from navigation equipment to correct the ADCP horizontal velocity field for possible alignment errors. Greenwood et al. (1993) examined deviations between actual and ADCP directions to known station locations to correct for local compass variations due to metal on board a ship. While Joyce (1989) proposed an amplitude correction for the horizontal velocities (his  $\beta$ ) attributed to sensor misorientation, this paper is the first, to our knowledge, that outlines a direct procedure for correcting vertical misalignment of the ADCP head. It will be organized in the following manner. Section 2 will contain the justification and theory for the rotation to be applied to the data. Section 3 will present the rotated velocity field, and the results will be discussed in section 4.

**2. Theory**

In many coastal regions, tidal currents dominate the velocity field. For regions of flat-bottom topography, the correlation between the vertical and horizontal tidal velocities can be shown to be 0.0. The barotropic component of the vertical velocity of the shallow water tidal wave, to the first order, is of the form

$$w = \frac{(z + H)}{H} \frac{\partial \eta}{\partial t}, \tag{2}$$

where  $\eta$  is the surface elevation, and  $z = -H$  at the bottom. The maximum amplitude of the surface tide is  $|\eta| = \omega \eta$ , where  $\omega$  is the dominant tidal frequency. For a typical tidal range of 2 m at the semidiurnal frequency, the expected maximum vertical velocity is  $0.3 \text{ mm s}^{-1}$ , well below the detection limit of the ADCP. Thus, the measured velocity field for barotropic tidal motion is horizontal.

Internal waves and baroclinic tides are associated

with large vertical velocities. For shallow water waves (e.g., Marsden and Greenwood 1994), the vertical and horizontal motion can be decomposed into normal modes:

$$[u_n(x, y, z, t), v_n(x, y, z, t)] = [U_n(x, y), V_n(x, y)]\phi_n(z)e^{-i\omega t} \tag{3a}$$

and

$$w_n(x, y, z, t) = W_n(x, y)\psi_n(z)e^{-i\omega t}. \tag{3b}$$

The vertical dependencies are related through

$$k_n \phi_n = \frac{d\psi_n}{dz},$$

where  $k_n \text{ (m}^{-1}\text{)}$  is a separation constant. The vertical dependence of the product of the vertical and horizontal velocity can be integrated from the bottom to the surface:

$$\int_{-H}^0 \psi_n \phi_n dz = \int_{-H}^0 \psi_n \frac{d\psi_n}{dz} dz = \frac{1}{2}[\psi_n^2(0) - \psi_n^2(-H)]. \tag{4}$$

Appropriate boundary conditions are  $\psi_n(-H) = 0$  at a flat bottom and  $d\psi_n(0)/dz - \psi_n(0)/h_n = 0$  at the sea surface, where  $h_n$  is the equivalent depth (see Leblond and Mysak 1978, 70). To a high degree of accuracy the surface boundary condition can be replaced by  $\psi_n(0) = 0$  (Gill 1982, 162). Thus, the depth integral of the horizontal and vertical velocities for linear internal waves is 0.0. Consequently, it is critical that measurements be obtained over the entire water column. If one has a sufficient sampling density in the vertical, as provided by a VM ADCP in bottom track mode, then the theoretical depth-integrated velocity cross-correlation matrix **A** for tidal flow should be of the form

$$\mathbf{A} = \begin{pmatrix} \langle u^2 \rangle & \langle uv \rangle & 0 \\ \langle uv \rangle & \langle v^2 \rangle & 0 \\ 0 & 0 & \langle w^2 \rangle \end{pmatrix}, \tag{5}$$

where the brackets indicate depth integration. It can be readily shown that one of the theoretical eigenvectors **e** of **A** will be vertical, that is, of the form **e** = [0, 0, 1].

In practice, for data contaminated with ship motion due to transducer misalignment, none of the eigenvectors will be vertical. However, one of the eigenvectors will indicate a local vertical direction and its associated eigenvalue will be the depth-averaged variance of the vertical velocity  $\langle w^2 \rangle$ . The data can then be rotated so that a new vertical axis lies along the direction of the eigenvector associated with the smallest eigenvalue of the velocity cross-correlation matrix. Let **e<sub>d</sub>** = [*e*<sub>1</sub>, *e*<sub>2</sub>, *e*<sub>3</sub>] be the eigenvector selected as corresponding to the vertical direction and **X** be a data matrix given by

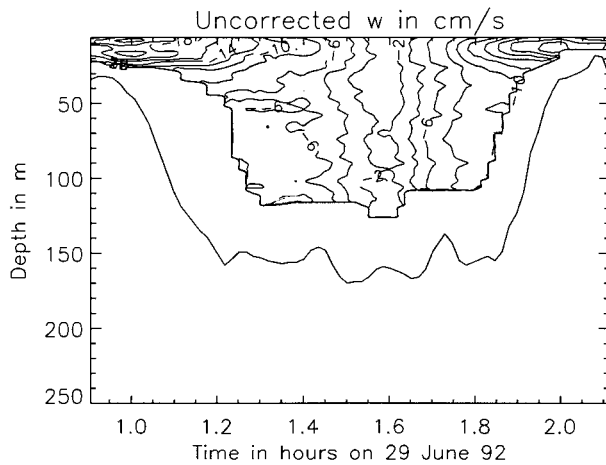


FIG. 1. Contour of isotachs (2.0 cm s<sup>-1</sup> interval) of vertical velocity. The bottom 15% of the data have been rejected due to sidelobe reflection. The initial sampling interval of 1.0 min has been smoothed using a 10.0-min boxcar filter. The solid line under the plot indicates the actual bottom topography. Note the large (~8 cm s<sup>-1</sup>) vertical velocities from the surface to the bottom over much of the data.

$$\mathbf{X}_n = (u_n, v_n, w_n),$$

where the subscript (*n*) refers to a depth value and

$$\mathbf{A} = \mathbf{X}^T \mathbf{X}.$$

Then, a new data matrix  $\mathbf{X}'$  can be formed by the double rotation

$$\mathbf{X}' = \mathbf{X} \begin{pmatrix} c_2 & 0 & s_2 \\ 0 & 1 & 0 \\ -s_2 & 0 & c_2 \end{pmatrix} \begin{pmatrix} 1 & 0 & 0 \\ 0 & c_1 & s_1 \\ 0 & -s_1 & c_1 \end{pmatrix},$$

where

$$c_1 = \cos\theta_1 = \frac{(e_1^2 + e_3^2)^{1/2}}{(e_1^2 + e_2^2 + e_3^2)^{1/2}},$$

$$s_1 = \sin\theta_1 = \frac{e_2}{(e_1^2 + e_2^2 + e_3^2)^{1/2}},$$

$$c_2 = \cos\theta_2 = \frac{e_3}{(e_1^2 + e_3^2)^{1/2}},$$

and

$$s_2 = \sin\theta_2 = \frac{e_1}{(e_1^2 + e_3^2)^{1/2}}.$$

The rotated product  $\mathbf{A}' = \langle \mathbf{X}'^T \mathbf{X}' \rangle$  will have  $z'$  axis aligned along  $\mathbf{e}_n$ , and  $\mathbf{A}'$  will be of the form given in Eq. (5). Since matrix multiplication is not commutative, the rotation about axis one followed by axis two will not have the same angular values as given above. The net effect is, however, independent of order of rotation and is to produce a cross-correlation matrix of the form of Eq. (5). Indeed, the programs were checked by ensuring that calculating the rotated cross-correlation matrix directly and ensuring that the appropriate off-di-

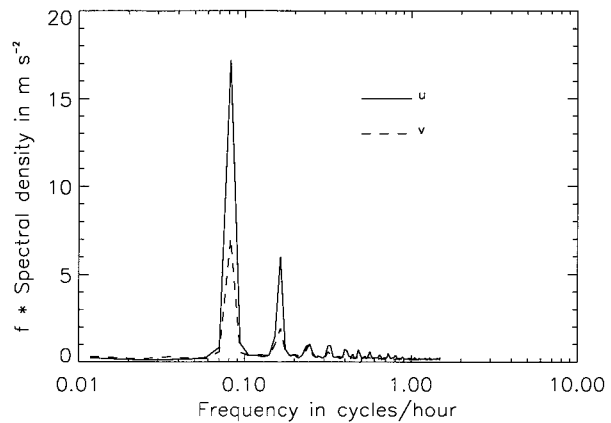


FIG. 2. Power spectral density of the *u* (along channel) and *v* (across channel) velocity. The data were ensemble averaged in 37 groups of 256 data points giving 95% confidence limits of (0.73, 1.47) times the spectral density value, assuming data independence. Note the dominance of the semidiurnal tide.

agonal terms were small. Care must be taken, however, if one is applying permanent corrections to manufacturer-supplied program packages such as RDI's DAS or Transect. In these cases, the order of rotation that the manufacturer used in the programs should be verified prior to calculating and applying corrections.

### 3. Data analysis

Data were collected from 20 to 30 June 1990 at the head of the Laurentian Channel, using a 150-kHz ADCP. The instrument was set with a 2-m bin size, sampling 1-min intervals. Typically, 75 samples were obtained per ensemble giving a nominal rms error of 2.20 cm s<sup>-1</sup> in *u* and *v* and 1.27 cm s<sup>-1</sup> in *w*. The data were further averaged for presentation using a 10-min running mean. Of particular interest is a section sampled from 0048 (0.8) to 0215 (2.25) UTC 29 June 1990 for which a contour plot of *w* is shown in Fig. 1. In the deep (150 m) portion, the isotachs show a distinct vertical orientation, and the large values of up to -8 cm s<sup>-1</sup> from the surface to the bottom that are clearly unrealistic. Large intense values of up to -20 cm s<sup>-1</sup> appear near the surface at the shelf break, but the unrealistic *w* contours over the flat-bottom topography cast doubt on the accuracy of the entire dataset. The persistent downward velocity would be consistent with an ADCP tilted upward toward the stern of the ship.

To correct the data, one must have a tidally dominated flow over a flat bottom. Figure 2 shows the power spectral density of the *u* (along channel) and *v* (across channel) velocities of a current meter moored at 20-m depth in the region for the period 6 May to 28 September 1990 (see Laforet 1994 for a complete data description). The flow is clearly dominated by the semidiurnal tide. Figure 1 shows that the ship passed over a region of relatively

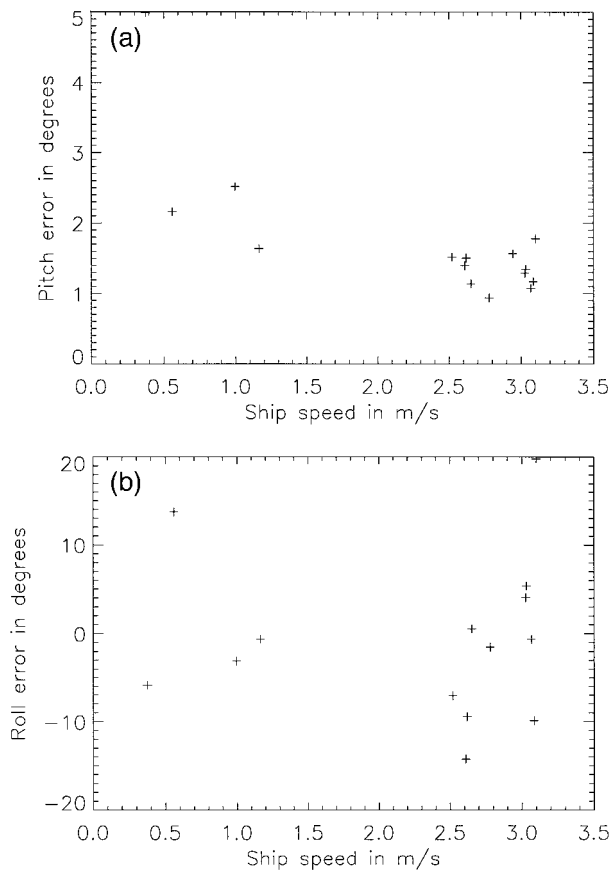


FIG. 3. (a) Pitch and (b) roll errors, respectively, as a function of ship speed based on a correction for each 1.0-min sample over the flat portion of the topography.

flat bottom from 0118 (1.3) to 0148 (1.8) UTC. Consequently, at least a portion of the data can be corrected.

Errors result from the physical misalignment of the transducers relative to the pitch and roll axes of the vessel. Since the data were recorded relative to north, they had to be converted back to a coordinate system relative to the ship. Consequently, the ship bottom track velocities were added to the recorded velocities and then rotated along the bottom track direction so that the data were oriented with the  $x$  and  $y$  axes along and across the ship, respectively, and the  $z$  axis oriented vertically upward. The velocity cross-correlation matrix given in Eq. (5) was calculated, and the positive  $z$  direction was assumed to be in the direction of the eigenvector corresponding to the minimum eigenvalue. The data were

rotated about the  $x$  and  $y$  axes so that the corrected vertical axis aligned with this direction. The horizontal velocities relative to the ship were then reoriented to along- and across-channel and the bottom track velocities subtracted to produce velocities relative to the earth.

Errors in orientation were calculated over the flat-bottom sectors of the cruise track for each 1-min ensemble. Figures 3a and 3b show the pitch and roll errors, respectively, as a function of ship speed. Errors in the pitch direction are constant at about  $1.2^\circ$  for ship speeds greater than  $2 \text{ m s}^{-1}$ . For ship speeds less than  $1 \text{ m s}^{-1}$ , the mean error increases to about  $2.0^\circ$ . The apparent roll error shows considerably more scatter with most values lying between  $\pm 10^\circ$ . This large scatter can be explained in terms of signal-to-noise considerations. Stochastic errors in VM ADCPs are determined by the number of pings measured, system configuration (RDI 1989), and fluctuations in the local environment, such as ship motion due to surface gravity waves, not corrected by the system. Greenwood et al. (1993) estimated actual stochastic errors to be a factor of four larger than those specified by RDI. A reasonable stochastic error in the vertical velocity for this study is about  $0.05 \text{ m s}^{-1}$ . The signal is the strength of the measured current relative to the ship—about  $3.0 \text{ m s}^{-1}$  in the pitch direction and  $0.25 \text{ m s}^{-1}$  in the roll direction. An expected stochastic error is  $\pm \tan^{-1}(0.05/0.25) = \pm 11^\circ$  in the roll direction, while only  $\pm \tan^{-1}(0.05/3.0) = \pm 1.0^\circ$  in the pitch direction, with increasing variability at lower ship speeds. These estimates are reflected in the data. The mean value of the roll errors, however, is near  $0^\circ$ . There is no evidence of a systematic variation in error for either the pitch or roll directions, suggesting that there was no increase in misalignment with ship speed. We will assume that the errors result from a fixed misorientation of the transducer and that a single bulk correction, based on all the measurements taken over the flat region of the transect, can be applied to all the data, including those collected over the slope. In effect, the flat-bottomed portion of the cruise track will be used to calibrate the instrument for the entire section.

A single rotation was calculated for the data obtained between 0118 (1.3) and 0148 (1.8) UTC. The initial and final matrix elements along with the associated eigenvalues and largest eigenvector are given in Table 1. The correction was found to be  $1.27^\circ$  and  $0.84^\circ$  in the pitch and roll directions, respectively. Since the ship velocity was approximately  $3.0 \text{ m s}^{-1}$ , the induced  $U \sin\theta$  error

TABLE 1. Results of the rotation of the  $\mathbf{A}$  matrix of Eq. (5) for the bulk correction. The matrix elements and eigenvalues are in centimeters squared per seconds squared. Pitch correction:  $1.27^\circ$ . Roll correction:  $0.84^\circ$ .

	$\langle u^2 \rangle$	$\langle v^2 \rangle$	$\langle w^2 \rangle$	$\langle uv \rangle$	$\langle uw \rangle$	$\langle vw \rangle$
Initial	$1.57 \times 10^8$	444 456	95 541	$1.93 \times 10^6$	$-3.47 \times 10^6$	-36 539
Final	$1.58 \times 10^8$	444 457	19 128	$-1.93 \times 10^6$	-2.27	0.274
Eigenvalues	420 916	19 133	$1.58 \times 10^8$			
Eigenvector used	-0.022	0.015	-0.999			

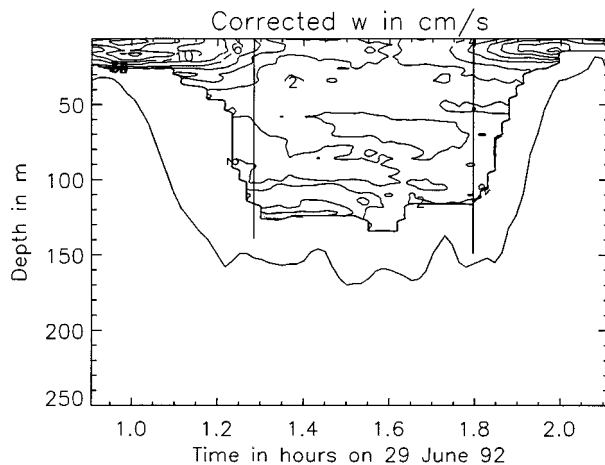


FIG. 4. Same as Fig. 1 after bulk corrections of  $1.27^\circ$  and  $0.84^\circ$  were applied in the pitch and roll directions, respectively. The two vertical lines indicate the time frame over which the corrections were calculated.

in the pitch direction was  $6.5 \text{ cm s}^{-1}$ , while a typical cross-ship flow was  $0.7 \text{ m s}^{-1}$  contributing a  $1.22 \text{ cm s}^{-1}$  error from the roll direction. Thus, even small errors in the pitch direction can create large systematic errors in the vertical velocity. A contour of the corrected vertical velocity appears in Fig. 4. The vertical lines indicate the region over which the rotation was calculated, although applied to the entire section. The isotachs of  $w$  are now oriented horizontally and are within two standard deviations of the expected error of the instrument (i.e., within the expected noise level) over most of the section, including a large portion of the slope.

#### 4. Discussion and conclusions

In order for the method to be effective, it should not merely eliminate all vertical velocities but also retain estimates where large values are expected. For example, topographic slopes can act as generating regions for internal tides and supertidal internal and lee waves. For a sloping bottom, the barotropic tide can force the flow to follow the topography, causing the density field to oscillate vertically, and hence act as a source of baroclinic energy. Maximum generation occurs at regions where the bottom slope matches the slope of the characteristics given by

$$c = \frac{\omega^2 - f^2}{N^2(z) - \omega^2} = \frac{dh}{dx},$$

where  $N^2(z)$  is the buoyancy frequency,  $f$  is the Coriolis parameter,  $\omega$  the tidal frequency, and  $h(x)$  the bottom contour. Generation typically occurs at sharp breaks in topography such as escarpments and the continental shelf break, characterized by enhanced vertical velocities along the bottom, extending to the middle of the water column at the break region. A theory of internal tide generation can be found in Baines (1982). His Fig.

1 gives an example of expected internal wave generation including enhanced vertical velocities at the shelf break similar to regions of large  $w$ , shown in Fig. 4, at the break of the escarpment. Forrester (1973) has found evidence for large internal tides, and Mertz and Gratton (1990) report observations of 40–60-m internal waves in the region. The obvious generation region is the escarpment. Values of the vertical velocity shown in Fig. 4 are, however, reduced by about  $5 \text{ cm s}^{-1}$  from corresponding areas depicted in Fig. 1. The net effect of this single bulk correction is to reduce the vertical velocity to the noise level in the deep flat-bottomed portion of the section while retaining large vertical velocities at the break in slope of the escarpment where internal wave/tide generation is expected.

Should the ship be steaming in the direction of the tidal flow, it is possible that the  $\langle v^2 \rangle$  and  $\langle uv \rangle$  terms of matrix  $\mathbf{A}$  [Eq. (5)] will be small, and the eigenvector corresponding to the smallest eigenvalue will not indicate the local vertical direction. In this case, the proposed correction will be unrealistically large and hence readily identified. For the 1-min samples, one case of a rotation of  $39^\circ$  for the pitch was found. Here, the next largest eigenvector gave a realistic result and was used in place. Assuming that the rotations correct for a physically misaligned ADCP head, once an appropriate set of values have been found, they should be applicable for all locations and all portions of the tidal cycle.

In this paper a technique is proposed to postcorrect the vertical orientation of a vessel-mounted acoustic Doppler current profiler. When the ship is running at speed, small alignment errors [ $O(1^\circ)$ ] that are insignificant for moored instruments severely distort the vertical velocity. A correction is proposed that is applicable in tidally dominated flat-bottomed areas. Under these conditions, the barotropic vertical velocity is negligible, and the depth-averaged correlation between the baroclinic vertical and horizontal velocities is 0.0. Consequently, the eigenvector corresponding to the smallest eigenvalue generally indicates the vertical direction. The velocity data matrix can then be rotated so the new vertical axis aligns with this eigenvector. An example is given where the vertical velocity field was obviously contaminated by ship motion. Misalignments of  $1.27^\circ$  and  $0.84^\circ$  for the pitch and roll directions were found. The dominant contribution to the error in  $w$  was due to pitch misalignment. The data were corrected and the revised contour plot indicated small vertical velocities over the flat portion of the section while preserving plausibly large vertical velocities over the break in topography at the edge of the escarpment above the Laurentian Channel.

*Acknowledgments.* We would like to thank all persons who contributed to the success of the 3-yr COUPPB program. RFM was supported by the Academic Research Program of the Department of National Defence of Canada. Additionally, YG received support from the

National Science and Engineering Council and the Department of Fisheries and Oceans, Canada.

#### REFERENCES

- Baines, P. G., 1982: On internal tide generation models. *Deep-Sea Res.*, **29**, 307–338.
- Forrester, W. D., 1973: Internal tides in St. Lawrence estuary. *J. Mar. Res.*, **32**, 55–66.
- Gill, A. E., 1982: *Atmosphere-Ocean Dynamics*. Academic Press, 662 pp.
- Greenwood, K. C., R. F. Marsden, and J. R. Buckley, 1993: Intercomparison of an acoustic Doppler current profiler with cycle-sondes in Knight Inlet, British Columbia. *Atmos.–Ocean*, **31**, 297–318.
- Joyce, T. M., 1989: On in situ “calibration” of shipboard ADCPs. *J. Atmos. Oceanic Technol.*, **6**, 169–172.
- Laforet R. G., 1994: Oceanographic and acoustic implication of freshwater releases into the Laurentian Channel. M.S. thesis, Physics Department, Royal Roads Military College, Victoria, BC, Canada, 95 pp. [Available from Physics Department, Royal Military College of Canada, Kingston, ON K7K 7B4, Canada.]
- Leblond, P. H., and L. A. Mysak, 1978: *Waves in the Ocean*. Elsevier, 602 pp.
- Marsden, R. F., and B. A. Juszko, 1987: An eigenvector technique for the calculation of directional spectra from heave, pitch and roll buoy data. *J. Phys. Oceanogr.*, **17**, 2157–2167.
- , and K. C. Greenwood, 1994: Internal tides observed by an acoustic Doppler current profiler. *J. Phys. Oceanogr.*, **24**, 1097–1109.
- , R. Paquet, and R. G. Ingram, 1994: Currents under land-fast ice in the Canadian Arctic Archipelago. Part I: Vertical velocities. *J. Mar. Res.*, **52**, 1017–1036.
- , B. A. Juszko, and R. G. Ingram, 1995: Internal wave directional spectra using an acoustic Doppler current profiler. *J. Geophys. Res.*, **100**, 16 179–16 192.
- Mertz, G., and Y. Gratton, 1990: Topographic waves and topographically induced motions in the St. Lawrence estuary. *Oceanography of a Large Scale Estuary: The St. Lawrence*, N. Solverger and M. I. El-Sabh, Eds., Springer-Verlag, 94–109.
- RDI, 1989: Acoustic Doppler current profilers. Principles of operation: A practical primer. RD Instruments, San Diego, CA, 36 pp.
- Schott, F., and K. D. Leaman, 1991: Observations with moored acoustic Doppler profilers in the convection regime in the Golfe du Lion. *J. Phys. Oceanogr.*, **21**, 558–574.